DYNAMIC PROPERTIES OF SATURATED SAND UNDER CYCLIC LOADING CONDITIONS (MODELING OF SHEAR STRESS-STRAIN RELATIONS)

J.Yamashita (I)
M.Majima (II)
Y.Nagataki (II)
Presenting Auther: M.Majima

SUMMARY

On the basis of cyclic loading test results on saturated sand, the authors divised the shear stress-strain relations model of saturated sand in which the reduction of shear resistance by cyclic loading were considered. To verify this model was good or not, comparison was made between test results and calculated ones using this model when inputting real seismic waves to specimens. As a result, it became clear that this model could express dynamic behavior of saturated sand under cyclic loadings fairly well.

INTRODUCTION

On the assumption that a large scale earthquake occurs at sandy grounds, the authors have made an attempt at modeling the shear stress-strain relations of saturated sand in the process of liquefaction which is to be used for earthquake response analysis of the structures on sandy grounds. This time,in order to investigate the effects of the confining pressure, relative density, principal stress ratio, shear strain-history, etc. on dynamic properties of saturated sand,dynamic torsional shear test was performed using sinusoidal and random waves.

TEST SUMMARY

The test was performed using torsional cyclic loading triaxial apparatus. Specimens were 13.5cm height of hollow cylinder having outside diameter of 7.0cm and inside diameter of 3.0cm. Materials used in test were Toyoura Sand and Niigata Sand, and relative density(Dr) were 50% and 70%. Specific gravity (Gs), uniformity cofficient(Uc), the mean of grain size(D_{50}), void ratio(e) and grain size distribution curves of these sand are shown in Table 1 and Fig. 1.

Table 1 Properties of Test Materials

	Gs	Uc	D_{50} (mm)	Void Ratio, e			
				MAX	MIN	Dr=50	Dr=70
Toyoura Sand	2.641	1.62	0.182	0.982	0.608	0.795	0.720
Niigata Sand	2.724	2.17	0.460	0.900	0.559	0.730	0.661

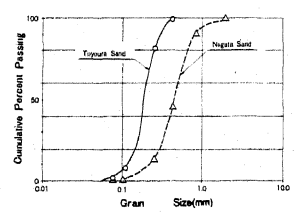

Fig. 1 Grain Size Distribution Curves of Test Materials

Test Procedures

After consolidating specimen at two kinds of principal stress ratio(σ'_3/σ'_1=0.5, 1.0), cyclic loading test was performed under undrained and strain controlled conditions using three types of waves as described later. The initial effective confining pressures(σ'_m)

(I) Manager of Foundation Engineering Section, Technical Research Institute, Taisei Corporation, Japan

(II) Research Engineer of Foundation Engineering Section, Technical Research Institute, Taisei Corporation, Japan

are 0.5, 1.0 and 2.0 kgf/cm^2 in case of Dr=50%, 0.5, 1.0, 2.0 and 4.0 kgf/cm^2 in case of Dr=70%. The back pressures are 0.5 kgf/cm^2 in all cases. Input waves are as follows;

Type I ---- The sinusoidal waves, which were kept shear strain amplitude(γ_d) constant, were input 30~50 cycles continuously at the frequency of 1Hz.

Type II --- Waves which were made by connecting the sinusoidal waves of different γ_d were input. As shown in Table 2, these were 9 kinds in all. The typical example is shown in Fig. 2.

Type III -- Waves which were transformed from the accelerogram of EL CENTRO and TOKACHI-OKI earthquake into displacement were input. Time history of these waves are shown in Fig. 3. Input level were controlled by γ_{max} in these figures.

Table 2 Kinds of Input Waves (Type II)

No.	N	Shear Strain Amplitude, γ_d($\times 10^{-4}$)
1	5	0.5→1.0→2.0→3.0→4.0→5.0→6.0→7.5
2	10	0.5→1.0→2.0→3.0→4.0→5.0→6.0→7.5
3	5	0.5→1.0→2.0→3.0→4.0→5.0→4.0→3.0→2.0→1.0→0.5
4	5	0.5→1.0→2.0→0.5→1.0→2.0→4.0→0.5→2.0→4.0→5.0
5	5	0.5→1.0→5.0→1.0→4.0→1.0→3.0→1.0→2.0→1.0→0.5
6	5	0.5→1.0→5.0→4.0→3.0→2.0→1.0→0.5
7	5 1	0.5→1.0→2.0→3.0→4.0→5.0 ↓↑ ↓↑ ↓↑ ↓↑ ↓↑ 0.25 0.5 0.75 1.0 1.25
8	5 1	0.5→1.0→2.0→3.0→4.0→5.0 ↓↑ ↓↑ ↓↑ ↓↑ ↓↑ 0.5 1.0 1.5 2.0 2.5
9	5 1	0.5→1.0→2.0→3.0→4.0→5.0 ↓↑ ↓↑ ↓↑ ↓↑ ↓↑ 0.75 1.5 2.25 3.0 3.75

N:Number of Cycles at The Same γ_d

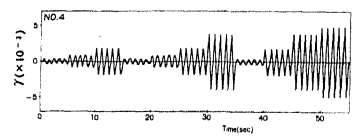

Fig. 2 Time History of Input Waves (Type II)

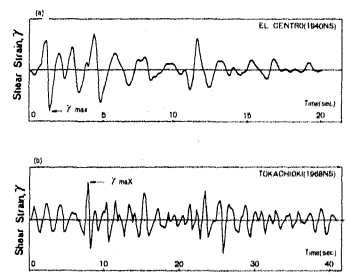

Fig. 3 Time History of Input Waves (Type III)

TEST RESULTS

τ-γ Relations

Fig. 4 shows an example of τ-γ hysteresis loops which were combined them at each γ_d using Type I. Fig. 5 shows skeleton curves which were jointed the vertex of the first cycle at each γ_d Fig. 6 shows an example of τ-γ hysteresis loops using Type II. Fig. 7 shows the mean of positive and negative vertex of the first and last cycle at each γ_d, which correspond to Fig. 6. The arrow head in Fig. 7 show loading sequence.

τ-γ Skeleton Curves

The relations between $\tau/(\sigma_m')^{0.9}$ (τ in Fig. 4 divided by $(\sigma_m')^{0.9}$) and γ are shown in Fig. 8. According to this figure, in case of the same Dr, the relations between $\tau/(\sigma_m')^{0.9}$ and γ can be expressed by Eq. 1.

$$\tau = v(\gamma)^w(\sigma_m')^{0.9} \qquad \text{----- (1)}$$

where v, w = the parameters which depend on properties of materials and Dr.

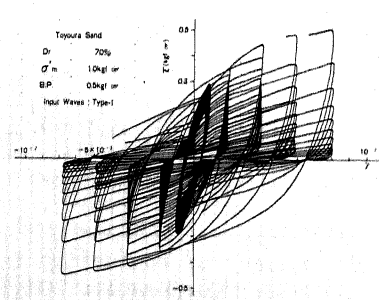

Fig. 4 τ-γ Hysteresis Loops (Type I)

The Effects of Number of Cycles on τ-γ Relations

In case of loading by Type I, the reduction ratio of shear stress amplitude(τ_d) with increase of number of cycles(N) increase as γ_d increase. Fig. 9 shows the relations between the ratio of shear stress amplitude of the Nth cycle to the first cycle(τ_N/τ_1) and N. According to Fig. 9, in

case of N=1.5 and $\tau_N/\tau_1 > 0.2$, τ_N/τ_1 are nearly proportional to log N. The gradients of straight lines (m) are different with materials, σ_m', Dr and γ_d, however, in case of not having been affected by shear strain-history, m are approximately proportional to log γ_d as shown in Fig.10. Thus, m-γ_d relations can be expressed by Eq. 2.

$$m = A \cdot \log \gamma_d + B \qquad \text{-----} \ (2)$$

On the other hand, Fig.11 shows the relations between the parameters A, B and σ_m' on Toyoura Sand, log A and log B are approximately proportional to log σ_m'. The same result was obtained on Niigata Sand. It follows from above that the relations between A, B and σ_m' can be approximated by Eq. 3.

$$A = a_1 \cdot (\sigma_m')^{a_2}$$
$$B = b_1 \cdot (\sigma_m')^{b_2} \qquad \text{-----} \ (3)$$

where a_1, a_2, b_1, b_2 = the parameters which depend on the properties of materials and Dr.

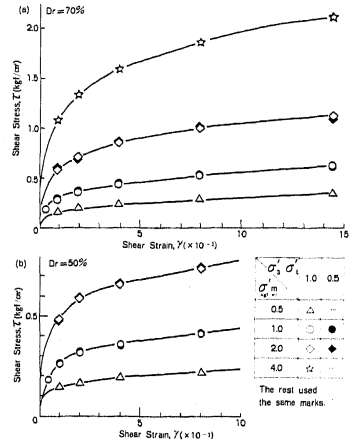

Fig. 5 τ-γ Skeleton Curves

The Effects of Shear Strain-History

The τ-γ relations are very different with dimensions of previous γ_d and their number of cycles even if the same materials, Dr and σ_m'. In a similar manner, the reductoin ratio of shear stress amplitude(m) which corrspond to γ_d are different with the type of shear strain-history. Still more, in case of having been subjected to larger strain γ_i than γ_d, τ_d and m are lower in comparison with them not having been subjected to γ_i even if the same γ_d. In case of cyclic loadings at the same γ_d, m using Type I are the greatest, and they decrease as γ_d/γ_i and τ_d/τ_s become lower. This fact, as is evident from shown later in Fig.14~Fig.16, is due to pore water pressure just before cyclic loading at arbitrary γ_d are different with γ_d and their number of cycles which specimens were subjected to previously. In other words, τ_d and m at arbitrary γ_d depend on the values of u/σ_m' and they become lower as the values of u/σ_m' increase even if the same γ_d.

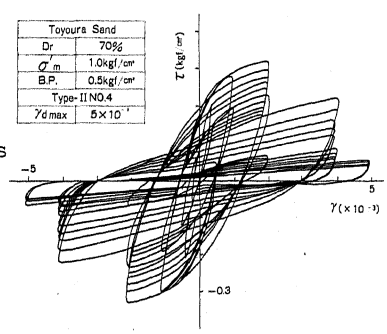

Fig. 6 τ-γ Hysteresis Loops (Type II)

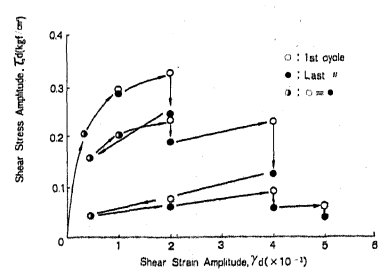

Fig. 7 τ_d-γ_d Relations (Type II)

The Shapes of Hysteresis Loops

The shapes of hysteresis loops change from spindle into slip form with the reduction of shear resistance and strain-hardening phenomenon occurs, which is caused by the positive dilatancy of soil particles and becomes more remarkable as σ_m', Dr and γ_d increase.

The Rules of History

As shown in Fig. 9, in case of loading by Type I, the gradient of straight

lines(m') which connect τ_1(N=1) and $\tau_{1.5}$ (N=1.5; number of cycles when the hysteresis curve get to the vertex of negative region at the first cycle) are nearly equal (0.4 ~ 0.5)m. Therefore, if not having been affected by shear strain-history, the relations between τ_1 and τ_N at the same γ_d can be expressed by Eq. 4.

$$N = 1.5 \quad \tau_{1.5} = (1 - m' \log 1.5)\tau_1 \qquad \text{--- (4)}$$
$$N \geq 2 \quad \tau_N = \{1 - m \log N + (m - m')\log 1.5\}\tau_1$$

On the other hand, according to the test results using Type II, when shear strain amplitude varied to γ_{d2} after loading N cycles at γ_{d1}, the first hysteresis curve at γ_{d2} proceeded to the vertex (γ_{d1}, $\tau_{(N+1)}$) of the (N+1)th cycle at τ_d. (Fig.12)

Relations between Damping Ratio(h) and γ_d

Fig.13 shows the h-γ_d relations using Type I at the first cycles. According to this figure, the maximum values of h are hardly different with Dr and σ_m'. They range from 0.38~0.42, and even if γ_d increase, h don't exceed their values. The range of shear strain where h are affected by σ_m' and Dr are the range where h are in less than the maximum value. On the other hand, as shown in Fig.13(b), h decrease with the reduction of shear resistance by cyclic loadings, and they approach 20% ultimately. That is to say, in case of loading N cycles at arbitrary γ_d, h can be approximated by Eq. 5.

$$h = (h_p - 0.2)\cdot\tau_d/\tau_s + 0.2 \qquad \text{----- (5)}$$

where h_p=damping ratio at γ_d which have not affected by cyclic loadings.

τ_s=shear stress on the skeleton curve at γ_d

The Tendencies of Pore Water Pressure Build-up

The typical tendencies of pore water pressure (u) build-up are shown in Fig.14~Fig.16. In case of loading by Type I, u build-up become more remarkable as σ_m' and Dr become lower and γ_d become larger. And the fluctuation amplitude of u increase as σ_m', Dr and γ_d increase. But, the gradients of u build-up and the fluctuation of u decrease gradually as u build-up. In a similar manner, in case of loading by Type II and Type III, the gradients of u build-up and their fluctuation amplitude increase as γ_d increase, and they decease as u build-up. That is to say, in case of cyclic loading at the same γ_d, u build-up and the fluctuation amplitude of u depend on u which accumulated previously. A noteworthy point is that u have twice as much frequency as τ and γ. At each cycle except

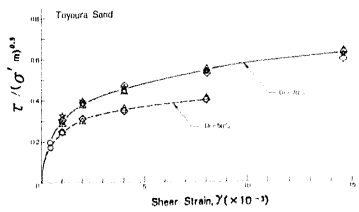

Fig. 8 $\tau/(\sigma_m')^{0.9}$-γ Relations

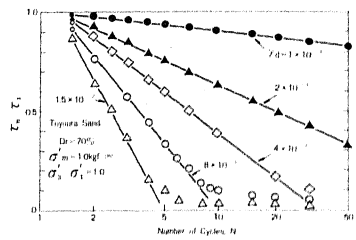

Fig. 9 τ_N/τ_1-log N relations

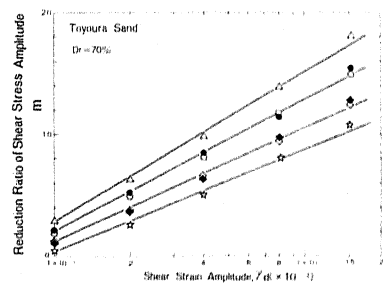

Fig. 10 m-log γ_d Relations

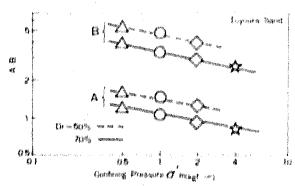

Fig. 11 log A, log B-log σ_m' Relations

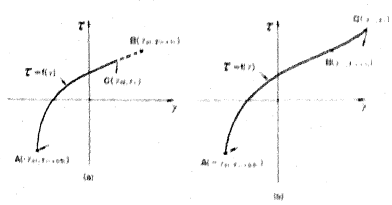

Fig. 12 The Rules of History

the first cycle, when γ and τ get to positive and negative vertexes u become the lowest, and when τ become nearly zero u become the greatest.

The Effects of The Confining Conditions

According to Fig. 5, Fig.10, Fig.13 and Fig.-16, σ_m' influence on the τ-γ skeleton curves, the m-γ_d relations, the h-γ_d relations and the tendecy of u build-up remarkably. On the other hand, in case of the same σ_m' even if the different principal stress ratio, it can be considered that there is no effect of them on dynamic properties. Excepting special ground as the ground in the vicinity of structure having spread foundation and slop, it is expected that σ_3'/σ_1' range from 0.5 to 1.0, so that it can be considered that the effects of confining conditions on dynamic properties can be evaluated by only σ_m'. Therefore, in the τ-γ relations model as described later, the effects of principal stress ratio isn't considered.

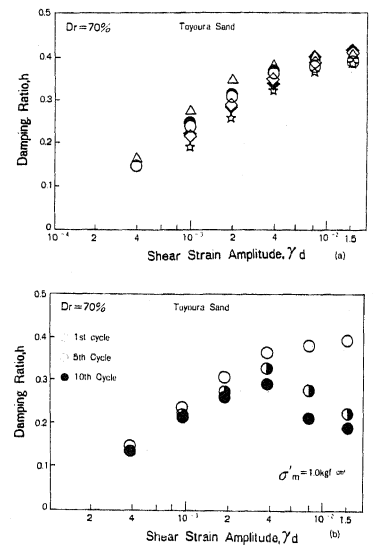

Fig. 13 h-log γ_d Relations (Type I)

FUNDAMENTAL THEORY OF ANALYZED MODEL

The model consists of the τ-γ skeleton curves, τ-γ hysteresis loops, h-γ_d relations, the reduction ratio of shear stress and the rules of history. In the sections that follows, the fundamental theory of this model is described.

τ-γ Skeleton Curves

Shear stress(τ_s) on skeleton curves at arbitrary γ are expressed by Eq. 6.

$$|\tau_s| = v \cdot |\gamma|^w \cdot (\sigma_m')^{0.9} \quad \text{-----} (6)$$

where v,w = the parameters which depend on the properties of materials and Dr.

In case of Dr=70% on Toyoura Sand, v≒2.08 and w≒0.28. Substitution of these values into Eq. 6, the skeleton curves correspond to σ_m'=0.5,1.0,2.0,4.0 kgf/cm^2 are shown in Fig.17.

τ-γ Hysteresis Loops

As shown in Fig.18, in case of assuming arbitrary two vertexes(γ_1,τ_1),(γ_2,τ_2)of hysteresis loop, the τ-γ relations of any point on this loop are expressed by Eq. 7.

$$\frac{\tau-\tau_0}{\tau_1-\tau_0} = \alpha\left(1\pm\frac{1}{2}\right)\left(\frac{\gamma-\gamma_0}{\gamma_1-\gamma_0}\right)^4 + \beta\left(\frac{\gamma-\gamma_0}{\gamma_1-\gamma_0}\right)^3 \pm\left(-\frac{\alpha}{2}\right)\left(\frac{\gamma-\gamma_0}{\gamma_1-\gamma_0}\right)^2 + (1-\beta)\left(\frac{\gamma-\gamma_0}{\gamma_1-\gamma_0}\right) - \alpha \quad \text{-----} (7)$$

$$\gamma_0=(\gamma_1+\gamma_2)/2 \ , \quad \tau_0=(\tau_1+\tau_2)/2$$

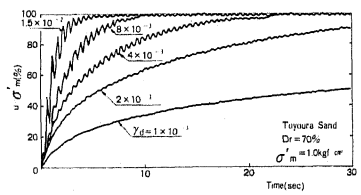

Fig. 14 Time History of Pore Water Pressure (Type I)

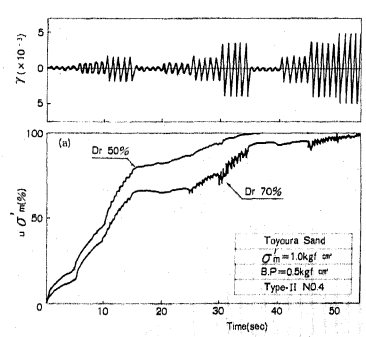

Fig. 15 Time History of Pore Water Pressure (Type II)

The parameters(α) stands for how a swell of curves and can be expressed by Eq. 8.

$$\alpha = 15\cdot\pi\cdot h/(24\pm2) \qquad \text{----- (8)}$$

($1-\beta$) stands for the gradient ratio between tangent which touches the hysteresis loop at the point corresponds to γ_0 and straight line which connects two vertexes in hysteresis loop. On the basis of test results, the parameter(β) can be expressed by Eq. 9 as a function of γ_d.

$$\beta=0.8-(2.4\times10^{-3})/(\gamma_d+3.0\times10^{-3}) \qquad \text{--- (9)}$$

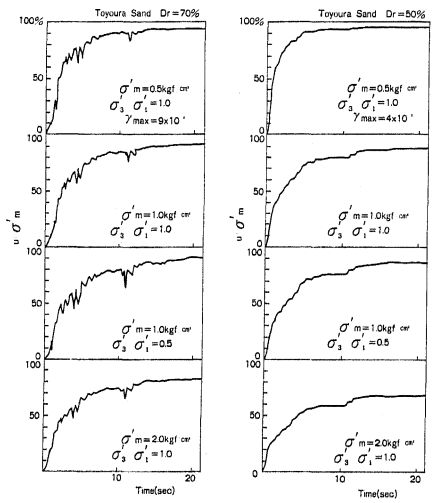

Fig. 16 Time History of Pore Water Pressure (Type III, EL CENTRO)

h-γ Relations

Damping ratio which have not been influenced by cyclic loadings are named h_p. h_p-γ_d relations are expressed by Eq.10.

$$\begin{aligned} &\gamma_d \leqq 1\times10^{-4} \text{ --- } h_p=0.05 \\ &1\times10^{-4} \leqq \gamma_d \leqq \gamma_h \text{ --- } h_p=\frac{\log\gamma_d-\log10^{-4}}{\log\gamma_d-\log10^{-4}}+0.05 \\ &\gamma_d \geqq \gamma_h \text{ --- } h_p=0.4 \end{aligned} \qquad \text{----- (10)}$$

γ_h in Eq.10 stands for shear strain amplitude when h_p getting to the maximum value(= 0.4), and is given by Eq.11.

$$\gamma_h = \gamma_{h1}\cdot(\sigma_m')^{0.5} \qquad \text{-------- (11)}$$

where $\gamma_{h1}=\gamma_1$ correspond to $\sigma_m'=1.0\text{kgf/cm}^2$

The h_p-γ_d relations on Toyoura Sand (Dr=70%) are shown in Fig.19. On the other hand, **h** which have been influenced by cyclic loading are expressed by Eq. 5 as a function of h_p and τ_d/τ_s. However, in case of $h_p \leqq 0.2$, it is assumed that $h=h_p$.

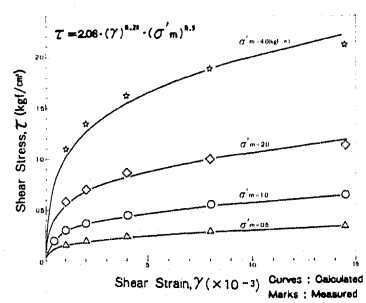

Fig. 17 τ-γ Skeleton Curves

The Rules of History

In case of assuming that the hysteresis loops proceed to next vertex(γ_2,τ_2) after turning over arbitrary vertex(γ_1,τ_1), γ_1-γ_2 relations and τ_1-τ_2 relations are expressed by Eq.12. (Strictly, their relations are modeled in twenty cases.)

$$\begin{aligned} \gamma_2 &= -\gamma_1 \\ \tau_2 &= -\tau_1(1-m\cdot\log 1.5) \end{aligned} \qquad \text{----- (12)}$$

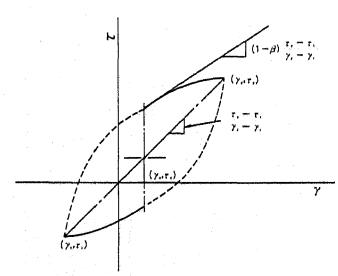

Fig. 18 τ-γ Hysteresis Loop

In the case that the shear resistance have not been reduced, in other words, if τ_1 are situated on the skeleton curve, **m** is calculated by Eq. 1 and Eq. 2. On the other hand, in case of the shear resistance having been reduced, **m** in Eq.12 is revised by Eq.13 according to the value of τ_1/τ_s.

$$m_1 = (1- |\log \tau_1/\tau_s|^{1.3})\cdot m \qquad \text{----- (13)}$$

More over, in case of having been subjected to larger strain than γ_1, m is reduced 20~50% according to the value of τ_1/τ_s.

COMPARISON BETWEEN TEST AND CALCULATED RESULTS

To verify whether this model is good or not, comparisons were made between test and calculated results on the value of shear stress response which were obtained from inputting the waves of Type III. Fig.20 and Fig.21 show the comparison on a part of τ-γ hysteresis loops and on the shear stress response. According to these figure, there are a little different between test and calculated results in the tendencies of shear stress reduction and in shapes of the hysteresis loops, however, it seems that this model can simulated the reduction properties of τ by cyclic loadings as appears in test results. Please note that each variable number used for analysis is shown in Table 3.

EARTHQUAKE RESPONSE ANALYSIS

Earthquake response analysis were performed using this model on imaginary sandy ground.
It was assumed that the sand deposit was 24m in depth and was 1.8 t/m^3 in density, the layer from G.L.±0m to -16m was 50% in relative density, the layer from G.L.-16m to -24m was 70% in relative density, the ground water level was G.L.±0m. The multi-shear-model was used for analysis and the deposit was divided into six layers(each layer was 4m in thikness). On the other hand, it was assumed that the viscous daming factor was proportional to instantaneous stiffness and its value was 0.02. Wilson's θ Methd was used for calculation and integral interval was 0.01 of a second. The fundamental natural period of this deposit was 0.41 of a second. Taft earthquake was chosen as input accelerogram because this earthquake contained a component of a time period about 0.41 of a second. The maximum value of input accelaration at base-rock was established at 138gal so that the maximum response value might

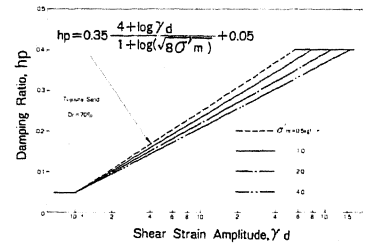

Fig. 19 h_p-log γ_d Relations

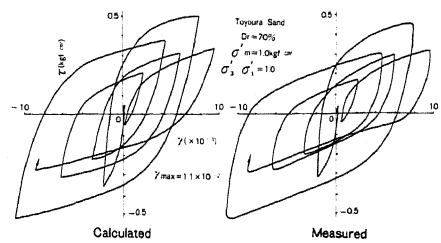

Fig. 20 τ-γ Hysteresis Loops (Type III, EL CENTRO)

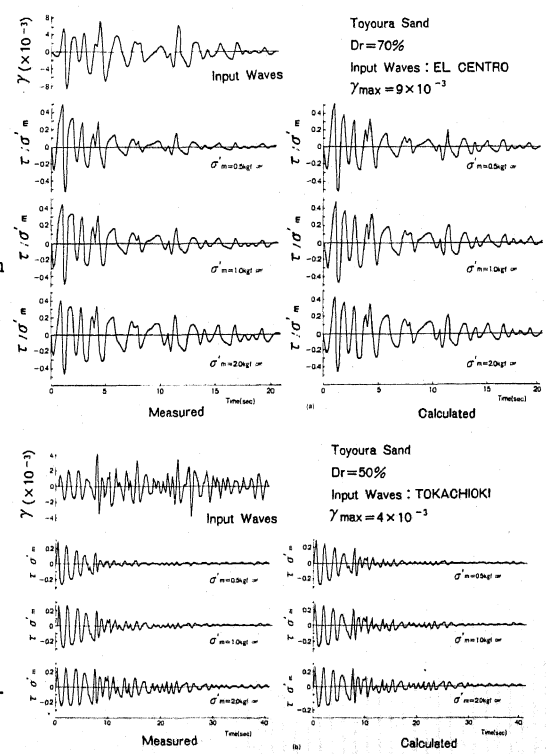

Fig. 21 Time History of γ and τ/σm'

be calculated about at 200gal at surface layer.

The Calculated Results

Fig.22 shows the response time history of shear stress, strain and acceleration at surface layer and input acceleration at base-rock. Fig.23 shows the response hysteresis loops at surface layer. According to these figures, the excellence of long time period component caused by the reduction of stiffness appears about 4 seconds later. The rapid increase of shear strain and the reduction of shear resistance ocurred about 6~7 seconds later, it seems that liquefaction began. Fig.24 shows distribution of the maximum response value of γ, τ and acceleration. At surface layer, γ became about 10^{-2}, liquefaction concentrated on this layer. The maximum response acceleration became 223gal, its response magnification became about 1.6.

CONCLUSIONS

As existing dynamics models on saturated sand, some effective stress methods for predicting pore water pressure build-up were proposed previously. The authors divised a new method for predicting the τ-γ relations using the reduction ratio of shear stress which were obtained from cyclic loadings test. It became clear that this model could express dynamic behavior of saturated sand under cyclic loadings fairly well and there is good prospect in using it for earthquake response analysis of structures on sandy ground.
Hereafter, the authors will investigate the adaptability of this model using earthquake accelerogram observed.

Table 1 Parameters Used for Analysis

Dr	V	W	a	a,	b	b,	/ar
[illegible]	[illegible]	[illegible]	[illegible]	[illegible]	[illegible]	[illegible]	[illegible]
[illegible]	[illegible]	[illegible]	[illegible]	[illegible]	[illegible]	[illegible]	[illegible]

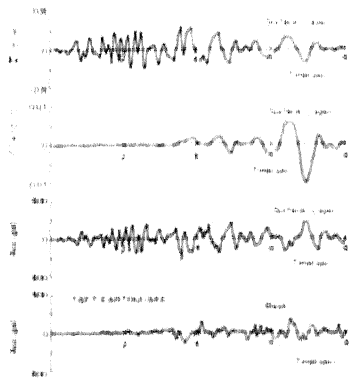

Fig. 22 Time History of Input and Response Waves

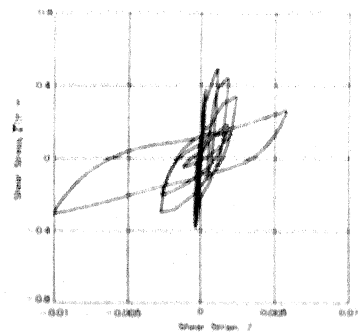

Fig. 23 τ-γ Hysteresis Loops at Surface Layer

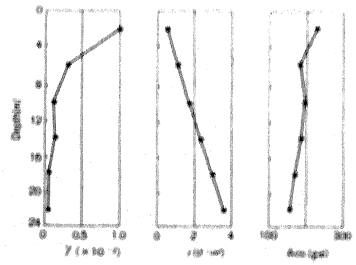

Fig. 24 Vertical Distribution of Maximum Response